IL NUOVO CIMENTO **41 C** (2018) 165
DOI 10.1393/ncc/i2018-18165-9

Colloquia: IWM-EC 2018

Hot news from INDRA and the scientific INDRA+FAZIA program at GANIL

O. Lopez on behalf of the INDRA-FAZIA Collaboration
Université de Caen Normandie, ENSICAEN, CNRS/IN2P3, LPC Caen - Caen, France

This contribution is dedicated to the memory of our late colleagues Marie-France Rivet and Elio Rosato.

received 3 December 2018

Summary. — We review some of the latest results obtained with INDRA 4π array in the Fermi energy domain. They concern isospin transport properties and N/Z equilibration for dissipative nuclear reactions, spinodal instabilities and phase transition in isospin-unbalanced systems for quasi-fused events, calorimetric studies for hot QP nuclei, and also about the improvement of the isotopic identification with INDRA Si-CsI telescopes. As a perspective, we also present and discuss the future experimental program planned at GANIL in the forthcoming years with the coupling between the multidetectors INDRA and FAZIA.

1. – Isospin transport around the Fermi energy

During the last years, the INDRA Collaboration have studied the isospin transport properties in nuclear reactions for systems corresponding to different isospins, here ^{124,136}Xe+^{112,124}Sn at $32A$ MeV. In the latest published paper by the INDRA Collaboration on this subject [1], we have investigated the isospin transport by looking at the abundance ratios for small clusters or light charged particles such as: d,t, ^{3}He, α, ^{6}He as a function of the centrality. The centrality selector is here the total transverse energy of light charged particles ($Z = 1, 2$) in the forward hemisphere in the centre of mass CM called $(\Sigma E_t)^{LCP}_{FwCM}$. Doing so, we also select particles/clusters for 2 differents angular domains, as presented in fig. 1, where we have plotted the abundance ratios (multiplicity of the particle of interest normalized to the proton one) for deuterons, triton, α particles and helium-6 as a function of the total transverse energy. The left panels correspond to particles emitted with $\theta_{CM} < 30$ degrees while the right ones correspond to $\theta_{CM} \geq 60$ degrees.

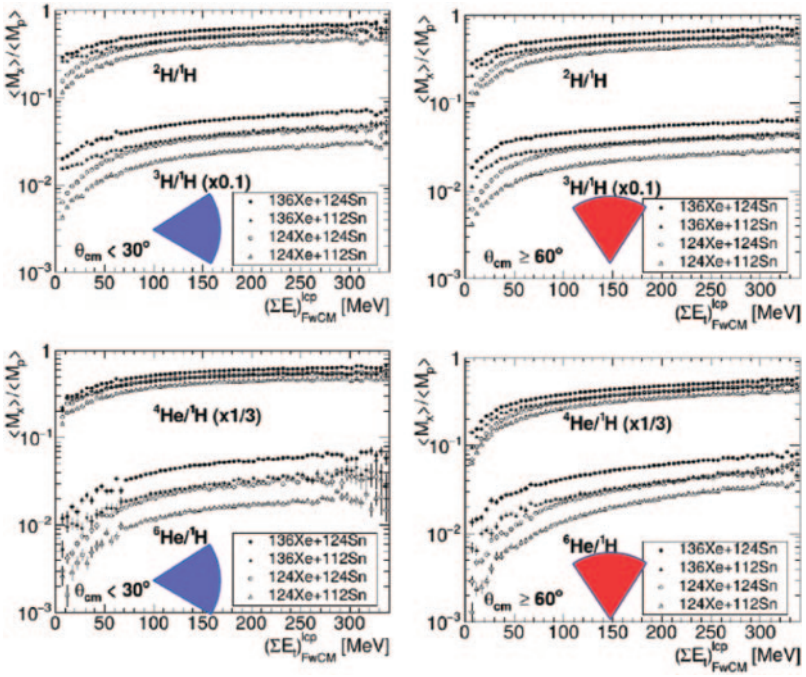

Fig. 1. – Abundance ratio for deuteron (top panels) and α particles (bottom) as a function of the total transverse energy for light charged particle in the forward CM hemisphere. Left: $\theta_{CM} < 30$ degrees. Right: $\theta_{CM} \geq 60$ degrees.

From fig. 1, we clearly see that the abundance ratios follow the N/Z of the corresponding systems; the highest the neutron richness, the larger the abundance ratio is. If we now look at the systems with the same total number of nucleons but different isospins: ^{124}Xe+^{124}Sn and ^{136}Xe+^{112}Sn, we notice that they overlap for $((\Sigma E_t)^{LCP}_{FwCM} > 200\,\mathrm{MeV}$, so for very dissipative and central collisions. This situation is readily observed whatever the *cm* emission angle. Thus, this suggests a complete chemical equilibration for these latters. It is worthwhile to mention that this is in contradiction with other works in the same incident range [2, 3].

The situation is opposite for ^{3}He clusters, where we observe a very distinct behaviour depending on the angular domain as presented in fig. 2. We notice that ^{3}He abundance ratios are insensitive to the entrance channel for the mid-rapidity region (right panel of fig. 2) and could be related to the specific time sequence for the emission of ^{3}He prior to any N/Z equilibration [4]. In any case, we do observe a chemical equilibration for these clusters, at variance with the others.

Another work performed within the INDRA Collaboration also investigates the isospin equilibration by looking at the ratio between tritons and ^{3}He ($A = 3$ clusters) for the same systems and is dicussed elsewhere in this conference [5].

2. – Spinodal decomposition in asymmetric nuclear systems

To study the isospin dependence of the phase diagram for nuclear matter, we have investigated high-order charge correlations as proposed in [6], here for the largest

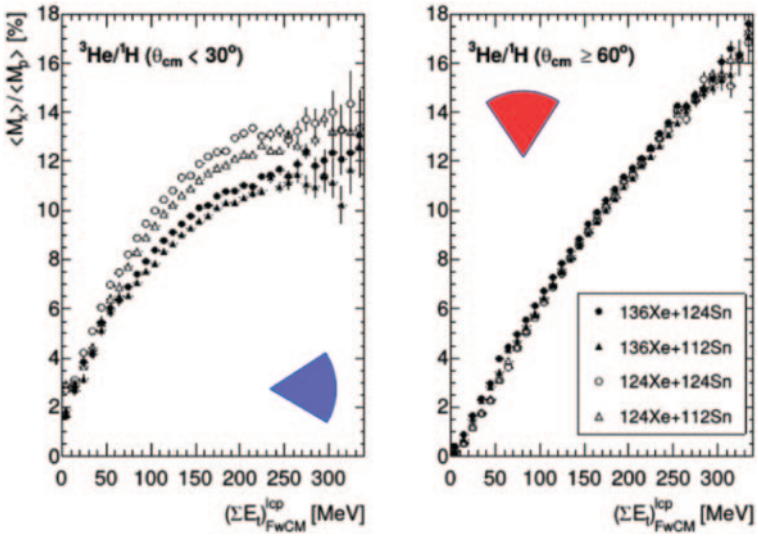

Fig. 2. – Abundance ratio for ^{3}He as a function of the total transverse energy for light charged particle in the forward CM hemisphere. Left: $\theta_{CM} < 30$ degrees. Right: $\theta_{CM} \geq 60$ degrees.

asymmetric systems available with INDRA: ^{124}Xe+^{112}Sn and ^{136}Xe+^{124}Sn at $32A$ and $45A$ MeV. Theoretical predictions with stochastic mean-field models show that density fluctuations hence spinodal decomposition should be reduced in asymmetric systems compared to more symmetric ones; this is due to the fact that the amplified fluctuations in nuclear matter within the spinodal region are of isoscalar and not isovector type [7]. To evidence the spinodal instabilities, we define higher-order charge correlations as the standard deviation: $\sigma_Z = \sqrt{\frac{1}{M}\Sigma_i^M (Z_i - \langle Z \rangle^2)}$, where M is the fragment ($Z > 5$) multiplicity, Z_i is the charge of the ith fragment, and $\langle Z \rangle = \frac{1}{M}\Sigma_i^M Z_i$ is the mean charge value for the event. We then build correlation functions $R(\langle Z \rangle, \sigma_Z) = Y_{corr}/Y_{uncorr}$ as the ratio between the correlated (true) yield Y_{corr} and the uncorrelated yield Y_{uncorr} built from a analytic multinomial distribution with intrinc probabilities [8]. The results concerning the charge correlations are shown in fig. 3 for ^{124}Xe+^{112}Sn at $32A$ MeV; we notice a significant over-correlation around $Z_{tot} = M \times \langle Z \rangle = 60$. This indicates the presence of equal-sized fragments, characteristics for the spinodal decomposition [6]. This signal is quite robust since the associated statistical confidence reaches 6–7σ [9].

The same analysis has been performed for all available systems at $32A$ and $45A$ MeV [9]. They are presented in table I. We notice that the more neutron-rich system ^{136}Xe+^{124}Sn always shows a reduction for events with equal-sized fragments as compared to the more proton-rich system, here ^{124}Xe+^{112}Sn. Secondly, when looking at the incident energy, we also notice a reduction of the number of events with equal-sized fragments between $32A$ and $45A$ MeV; these two findings are fully compatible with the scenario of spinodal instabilities triggered by isoscalar (density) fluctuations, where the dynamics of the collision covers fully the spinodal zone at $32A$ MeV, and only partially at $45A$ MeV [9].

The obtained results suggest that multiple-fragment production, often quoted as multifragmentation, can be attributed to mean-field fluctuations, and lead to the liquid-gas phase transition where the nuclear system moderatly excited and at low density can

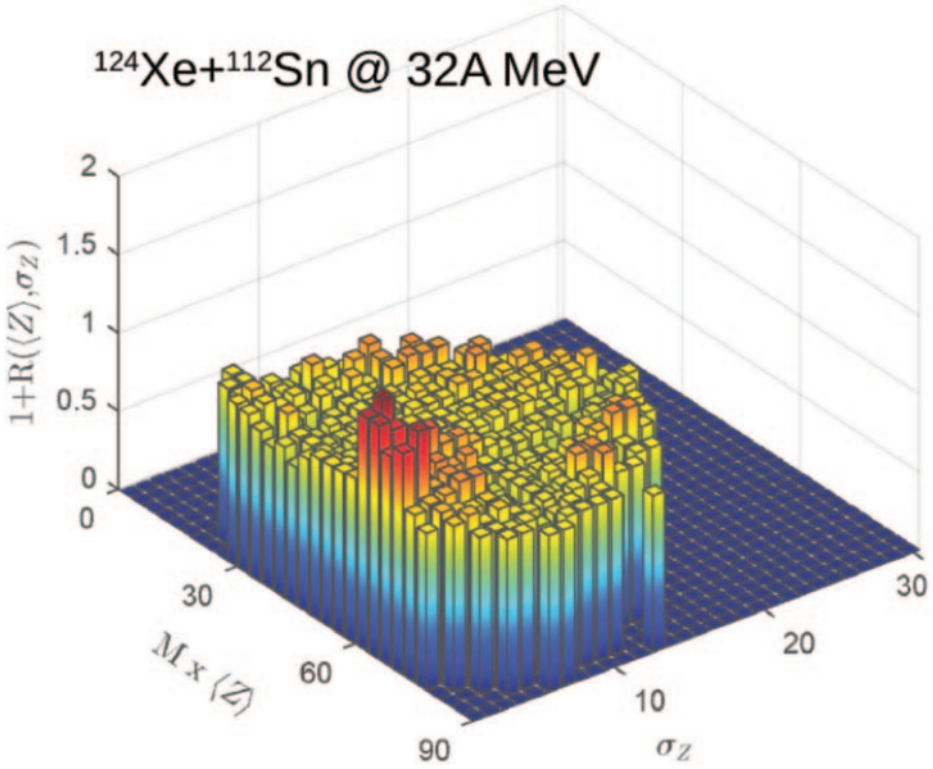

Fig. 3. – Correlation function in the plane $M\langle Z\rangle \times \sigma_Z$ for ^{124}Xe+^{112}Sn at 32A MeV. Taken from [9].

explore the spinodal region. If the time spent in this region is sufficient large to amplify the fluctuations, the system could break up in several pieces, possibly equal-sized. The characteristic time for such process is of the order of 100–150 fm/c. Combining these results with the ones obtained from the negative heat capacities, bimodalities or caloric curves [10], we believe that this could greatly help to solve the puzzle related to the fragment production in nuclear reactions around the Fermi energy.

TABLE I. – *Number of events and percentage for equal-sized fragments events, here with* $\sigma_Z < 2$. *The extra events give the number of over-correlated events as compared to the uncorrelated background. Taken from* [9].

E (AMeV)	System	Events	(%)	Extra events	(%)
32	^{124}Xe+^{112}Sn	1313	0.27	336	0.068 ± 0.004
32	^{136}Xe+^{124}Sn	1077	0.32	217	0.064 ± 0.004
45	^{124}Xe+^{112}Sn	1073	0.34	77	0.025 ± 0.003
45	^{136}Xe+^{124}Sn	68	0.030	15	0.0065 ± 0.0017

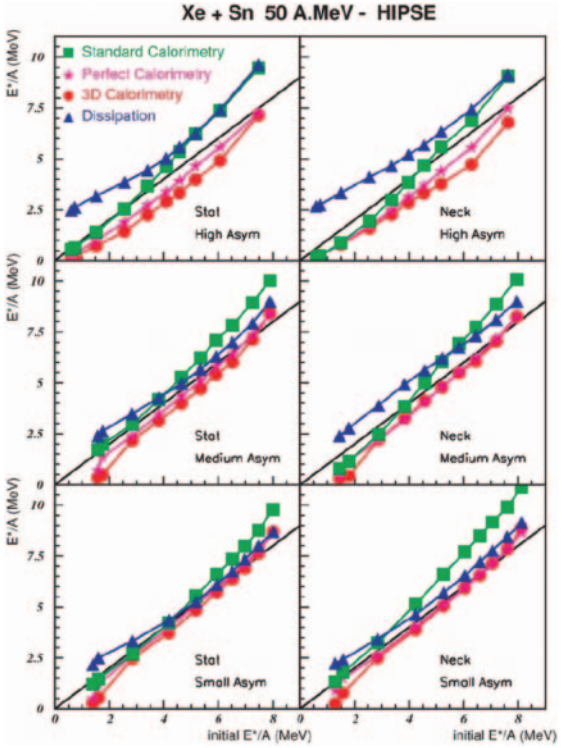

Fig. 4. – Simulation results from HIPSE. Excitation energy estimated by different calometric methods as a function of the true one. Taken from [12].

3. – 3D calorimetry for hot nuclei

As discussed previously, the phase transition for hot nuclei needs an accurate determination of the thermodynamic quantities such as density, temperature and excitation energy. In this context, the INDRA Collaboration has performed systematic comparisons between experimental data and the event generator HIPSE [11], for peripheral and semi-peripheral events, for reaction products emitted in the forward CM hemisphere, so mainly associated to the quasi-projectile (QP).

We present in fig. 4 the obtained excitation energy by different calorimetries for QP events as a function of the true one extracted from HIPSE. These method are all marked with uncertainties which can be as large as 15–20% depending on the reaction mechanism [12]. It is worthwhile to mention that standard calorimetry, which is done by doubling the contribution of particles in the forward QP hemisphere, give generally the worst measurement, except at very low excitation energy. The best method is the one called "3D calorimetry" which consists of taking a specific angular range in the QP forward hemisphere [13]. This method allows indeed to reduce the pollution coming from other sources such as the neck region or the quasi-target and accurately define caloric curves.

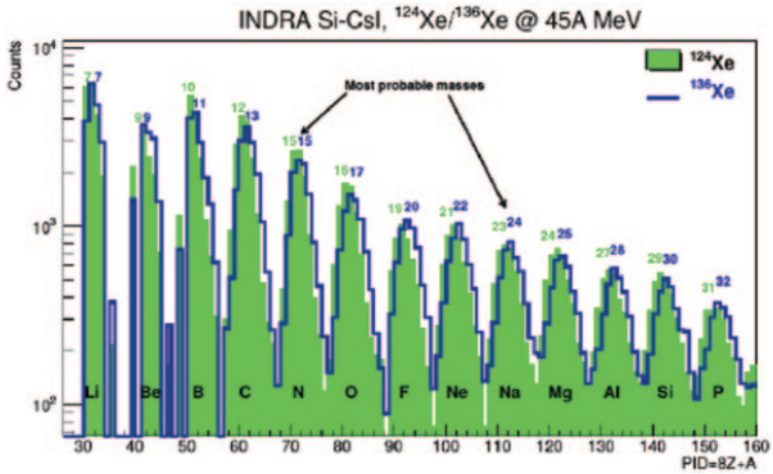

Fig. 5. – Isotopic distributions for the systems ^{124}Xe+^{124}Sn and ^{136}Xe+^{124}Sn at 45A MeV in INDRA Si-CsI telescopes. Taken from [14].

4. – Improving isotopic identification for Si-CsI telescopes

The INDRA Collaboration has recently developed a new identification scheme for Si-CsI telescopes such as the ones of INDRA [14]. The method relies on the description of the light signal induced by the punch-through of heavy ions in CsI(Tl) crystals described and used in [15]. Using this information together with the ΔE signal coming from the first silicon detector, we have been able to extend the usual isotopic identification performances for such INDRA telescopes from $Z = 6$–8 up to $Z = 15$.

This is here illustrated by fig. 5 where the isotopic distributions refer to two different systems, here ^{124,136}Xe+^{124}Sn at 45A MeV. We notice the isotopic distributions obtained up to $Z = 15$, together with a slight shift of 1–2 mass units between the 2 systems as expected from the Physics; here, we look at telescopes located between 2 and 45 degrees polar angle in the laboratory. Thus, they mainly record QP events, from light particles up to residues. It is then normal to get slightly different isotopic distributions. Moreover, by looking at quasi-elastic QP events, we have shown that the isotopic uncertainty for $Z > 15$ was under control and has been estimated to 2–3 mass units for $Z = 54$. These results show that the investigation concerning the isospin degree of freedom in nuclear reactions using INDRA can surely bring new information (isotopic distributions) in the next future by applying this improved identification scheme on Si-CsI telescopes.

5. – Scientific program for INDRA-FAZIA at GANIL

In the following years, the INDRA-FAZIA Collaboration would like to investigate the nuclear equation of state at low density in the isovector sector. A specific R&D program named FAZIA has been developed during the past years to improve the isotopic identification capabilities for reaction products in nuclear collisions around the Fermi energy. A detailed description of FAZIA specifications and performances can be found elsewhere in this conference [16, 17].

Heavy-ion induced reactions offer unique opportunities to probe nuclear properties far from the ground state [18]. More specifically at incident energies between 10 and

100 MeV/nucleon it is possible to investigate the thermal and mechanical properties of asymmetric ($N \neq Z$) nuclear matter [18]. Such reactions are a benchmark for studying dynamics of strongly-interacting N-body quantal systems, for which no fully consistent theoretical description yet exists [19]. Also, they are of paramount importance in the astrophysical context for the description of the core-collapse of supernovae, as well as the formation and static properties of proto-neutron stars [20, 21]. In this framework, the nuclear equation of state for uniform matter

$$E\left(\rho, \delta = \frac{N-Z}{A}\right) \Big/ A = E_0(\rho, \delta = 0) + E_\delta(\rho, \delta)$$

constitutes one of the most important topics for Nuclear Physics and is still extensively investigated nowadays. This equation is valid for uniform matter and need to be modified in case of heteregeneous matter with clusters. This last point will be the subject of a forthcoming proposal concerning the study of clusterisation in dilute nuclear matter.

The isoscalar part of the EOS $E_0(\rho, \delta = 0)$ is well established from both experimental and theoretical studies, concerning the saturation density ρ_0, the saturation energy $E_0(\rho_0)$ and the isocalar incompressibility modulus K_0 [22] with respectively $\rho_0 = 0.155 \pm 0.005\,\mathrm{fm}^{-3}$, $E_0(\rho_0) = -15.8 \pm 0.3\,\mathrm{MeV}$, and $K_0 = 9{\rho_0}^2(\frac{\partial^2 E_0}{\partial \rho^2})_{\rho=\rho_0} = 240 \pm 20\,\mathrm{MeV}$. On the other hand, the isovector part $E_\delta(\rho, \delta)$ is less well known, and analyses with better sensitivity still need to be conducted to better constrain it [20, 22, 23]. This latter can be expressed in the parabolic approximation as: $E_\delta(\rho, \delta) = E_{sym}(\rho)\delta^2$ where $E_{sym}(\rho)$ is defined as the symmetry energy: $E_{sym}(\rho) = \frac{1}{2}(\frac{\partial^2 E_\delta(\rho,\delta)}{\partial \delta^2})_{\delta=0}$. Generally speaking, $E_{sym}(\rho)$ is developed in a Taylor series of the reduced density $x = (\rho - \rho_0)/(3\rho_0)$,

$$E_{sym}(\rho) = S + L_{sym}x + \frac{1}{2}K_{sym}x^2 + \cdots$$

considering here terms up to second order in x and with $S = E_{sym}(\rho_0)$, $L_{sym} = 3\rho_0 \frac{\partial E_{sym}(\rho)}{\partial \rho}|_{\rho_0}$, $K_{sym} = 9\rho_0^2 \frac{\partial^2 E_{sym}(\rho)}{\partial \rho^2}|_{\rho_0}$ respectively the symmetry energy, slope and curvature parameters at saturation density. Today, S is well constrained by static properties (nuclear masses, isobaric analog states,...) with $S = 32.7 \pm 1.5\,\mathrm{MeV}$. The slope parameter L_{sym} is still under evaluation, with a common accepted range $L_{sym} = 40$–$80\,\mathrm{MeV}$ [22]. The relative uncertainty is then larger than 30% while it is less than 5% for S. For the second order term K_{sym}, the situation is even worse with more than 100% uncertainty at the moment. As a matter of fact, the evaluation of these first terms of the Taylor expansion for $E_{sym}(\rho)$ are mandatory for Neutron Stars; for example, a variation of $\pm 20\,\mathrm{MeV}$ for L_{sym} could result in a variation of the Neutron Star radius of $\pm 1.5\,\mathrm{km}$ (the smaller L_{sym} is, the more compact is the Neutron Star) depending on the EOS [24]. For the moment, the radius of a canonical Neutron Star ($M_{NS} = 1.4 M_o$) is estimated at $R_{1.4} = 12.3 \pm 2\,\mathrm{km}$ from the last observational data available [24, 25], and a more accurate determination for L_{sym} and K_{sym} coming from Nuclear Physics will be greatly appreciated.

5˙1. *Physics case.* – As a first experiment, we present here the first of a series for the different physics cases presented in the Letter of Intent (LoI) at the GANIL PAC and SAC in 2014 [26]. For this first beam request, we want to probe the symmetry energy and its density dependence S, L_{sym}, K_{sym} by investigating isospin transport and

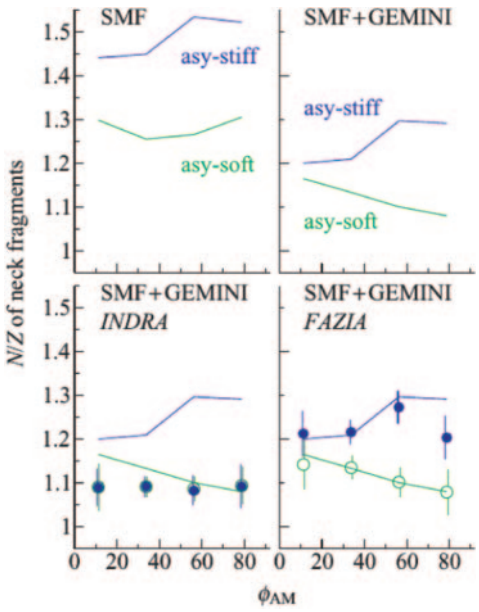

Fig. 6. – SMF calculations for ^{68}Ni+^{68}Ni at 40A MeV with asy-stiff (in blue) and asy-soft (in green) parametrizations for the isospin content and for neck fragments from ternary events. Upper left: hot primary fragments, upper right: cold secondary fragments after GEMINI, bottom left: cold secondary fragments filtred with INDRA, bottom right: cold secondary fragments filtered with FAZIA. Extracted from [30].

equilibration in dissipative reactions at around and above the Fermi energy [27, 28]. It is a part of the scientific program presented in the above-mentioned LoI [26].

From microscopic transport theories, in presence of isospin and density gradients ($\nabla\delta$ and $\nabla\rho$), proton and neutron currents j_n and j_p are known to depend on the symmetry energy and its density dependence [29]:

$$j_n - j_p \propto \delta\left(\frac{\partial E_{sym}}{\partial\rho}\right)\nabla\rho - \rho E_{sym}\nabla\delta. \tag{1}$$

The first term in the right hand side of eq. (1) is usually referred to as isospin migration or distillation depending on $\nabla\rho$ and the second one as isospin diffusion depending on $\nabla\delta$.

In non-central heavy-ion collisions in the Fermi energy domain a low-density "neck" of matter is transiently formed between projectile and target nuclei. By varying the N/Z ratio of the collision partners, we can vary the isospin gradient, while by modifying the incident energy we can change the density range, the timescale of the process and the degree of excitation of the matter through which the diffusion/migration occurs. This flow stops when the projectile and target reseparate and the "neck" breaks up into intermediate-mass fragments and light clusters. Detecting the A and Z of the reaction products as a function of their velocity then allows, after correcting for secondary decays, to "measure" the strength of the differential current $|j_n - j_p|$ and thus to access the different terms of eq. (1).

To illustrate this case, we present some Stochastic Mean-Field (SMF) simulations for ternary events (quasi-projectile+neck+quasi-target) obtained for the $^{58/68}$Ni+^{58,68}Ni

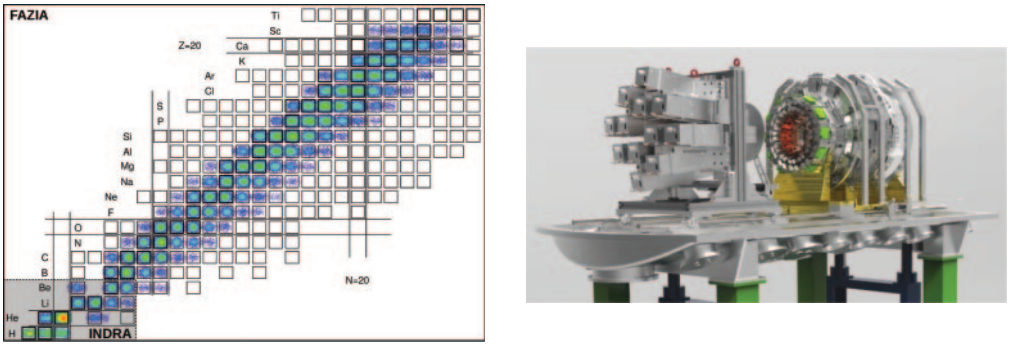

Fig. 7. – Left: Z-N identification map obtained with FAZIA, on the bottom left corner (grey area), the corresponding Z-N identification map obtained with INDRA. Right: coupling beween FAZIA (left) and INDRA (right) in the D5 scattering chamber at GANIL. The beam is coming from the right.

system at $40A$ MeV in fig. 6. Using two different parametrizations for the density dependence of the symmetry energy (asy-soft with $L_{sym} = 40$ MeV and asy-stiff with $L_{sym} = 80$ MeV) [30], we report in fig. 6 the isospin content (N/Z) as a function of ϕ_{AM} angle defined as the angle in the center of mass between the neck fragment and the direction given by the quasi-projectile and quasi-target. The two parametrizations give different results if we look at the upper left panel of fig. 6 where only hot and primary fragments are considered. If we now de-excite the primary fragments using GEMINI statistical model, we obtain the upper right panel of fig. 6 where the two parametrizations always display some differences, although the secondary emission reduces the effect. Now, if we filter by INDRA (fig. 6, bottom left) and FAZIA (fig. 6, bottom right) acceptances [31], we notice that only FAZIA still preserves the difference between the two parametrizations; this is due to the isotopic identification which is largely extended between INDRA and FAZIA.

Also, isoscaling of the largest fragment has been proposed sometime ago to evaluate the density dependence of the symmetry energy [32]. Isoscaling is a general scaling law observed in Heavy-ions induced reactions concerning the relative yield of a given cluster or fragment $Y(Z, N)$ for two similar reactions differing only by their isospin content [33]. The theoretical analysis discussed in [32] within the Lattice-Gas Model framework with an isospin + coulomb nuclear interaction has shown that the isoscaling for the largest fragment (quasi-projectile in our case) can be sensitive to the symmetry energy and its density dependence. This requirement corresponds exactly to the existing performances concerning isotopic identification deduced from our latest experiments with FAZIA telescopes [34].

5˙2. *INDRA-FAZIA experimental setup.* – The proposed experimental study has two main requirements: (1) A, Z identification and kinetic energy of as many reaction products as possible *in each event*, and therefore their velocity vector; (2) as close as possible to 4π coverage for complete event reconstruction, in order to ensure a good control of the reaction mechanism/impact parameter. This will be achieved by coupling the existing INDRA array with 12 blocks of FAZIA [31] as shown in fig. 7.

The FAZIA blocks will be placed at one metre from the target covering the polar angles from 1.5 deg. to 14 deg.. Each block consists of sixteen telescopes Si1-300 μm - Si2-500 μm - CsI(Tl)-10 cm thick. Each telescope is capable of unit mass and charge

resolution up to $Z \sim 20$–25, depending on energy [34-36]. For the reactions we propose to study, FAZIA will provide full charge and mass identification for most mid-rapidity products as well as for the majority of quasi-projectile residues and decay products.

The angles from 14 deg. to 176 deg. will be covered by INDRA telescopes, providing Z identification for all charged reaction products with low thresholds ($\sim 1\,\mathrm{MeV}/u$) thanks to a first stage composed of low pressure ionization chambers (from 14 to 88 deg. in this case). Isotopic identification is possible for high-energy light particles ($Z \leq 4$) punching through to the CsI(Tl) scintillator detectors which are the last stage of all telescopes. In addition, the use of thin ($150\,\mu$m) silicon detectors as second stage of the telescopes from 14 deg. to 45 deg. will increase the isotopic identification capabilities of INDRA up to $Z \leq 8$ at these angles [14], completing the coverage of the mid-rapidity region by FAZIA.

REFERENCES

[1] Bougault R. *et al.*, *Phys. Rev. C*, **97** (2018) 024612.
[2] Kelsis A. L. *et al.*, *Phys. Rev. C*, **81** (2010) 054602.
[3] Sun Z. Y. *et al.*, *Phys. Rev. C*, **82** (2010) 051603R.
[4] Jedele A. *et al.*, *Phys. Rev. Lett.*, **118** (2017) 062501.
[5] Henri M., these proceedings.
[6] Borderie B. *et al.*, *Phys. Rev. Lett.*, **86** (2001) 3252.
[7] Colonna M. *et al.*, *Phys. Rev. Lett.*, **88** (2001) 122701.
[8] Borderie B. *et al.*, *Eur. Phys. J. A*, **30** (2006) 243.
[9] Borderie B. *et al.*, *Phys. Lett. B*, **782** (2018) 291.
[10] Borderie B. and Rivet M. F., *Prog. Part. Nucl. Phys.*, **61** (2008) 551.
[11] Lacroix D., Van Lauwe A. and Durand D., *Phys. Rev. C*, **69** (2004) 054604.
[12] Vient E. *et al.*, arXiv:1707.01264 [nucl-ex] (2017).
[13] Vient E. *et al.*, arXiv:1804.07552 [nucl-ex] (2018).
[14] Lopez O. *et al.*, *Nucl. Instrum. Methods Phys. Res. A*, **884** (2018) 140.
[15] Parlog M. *et al.*, *Nucl. Instrum. Methods Phys. Res. A*, **482** (2002) 674.
[16] Gruyer D., these proceedings.
[17] Camaiani A., these proceedings.
[18] Durand D., Tamain B. and Suraud E., *Nuclear Dynamics in the Nucleonic Regime* (IOP, New York) 2001, 1 and references therein.
[19] Xu J. *et al.*, *Phys. Rev. C*, **93** (044609) 2016.
[20] Li B. A., Chen L. W. and Ko C. M., *Phys. Rep.*, **464** (2008) 113.
[21] Lattimer J. M. and Prakash M., *Science*, **304** (2004) 536.
[22] Li B. A. and Han X., *Phys. Lett. B*, **727** (2013) 276.
[23] Ademard G. *et al.*, *Eur. Phys. J. A*, **50** (2014) 33.
[24] Lattimer J. M., *Annu. Rev. Nucl. Part. Phys.*, **62** (2012) 1.
[25] Fattoyev F. J., Piekarewicz J. and Horowitz C. J., *Phys. Rev. Lett.*, **120** (2018) 172702.
[26] Letter of Intent, *N/Z dependence of the dynamics in dissipative collisions, from evaporation towards vaporization*, GANIL PAC (2014), `http://fazia.in2p3.fr/spip.php?article177`.
[27] Su Z. Y. *et al.*, *Phys. Rev. C*, **82** (2010) 051603R.
[28] Coupland D. *et al.*, *Phys. Rev. C*, **84** (2011) 054603.
[29] Baran V. *et al.*, *Nucl. Phys. A*, **703** (2002) 603.
[30] FAZIA Collaboration (Napolitani P. *et al.*), *Phys. Rev. C*, **81** (2010) 044619.
[31] Bougault R. *et al.*, *Eur. Phys. J. A*, **50** (2014) 47.
[32] Lehaut G., Gulminelli F. and Lopez O., *Phys. Rev. Lett.*, **102** (2010) 142503.

[33] Tsang M. B. *et al.*, *Phys. Rev. Lett.*, **86** (2001) 5023.
[34] FAZIA Collaboration (Carboni S. *et al.*), *Nucl. Instrum. Methods Phys. Res. A*, **664** (2012) 251.
[35] FAZIA Collaboration (Pastore G. *et al.*), *Nucl. Instrum. Methods Phys. Res. A*, **860** (2017) 42.
[36] FAZIA Collaboration (Gruyer D. *et al.*), *Nucl. Instrum. Methods Phys. Res. A*, **847** (2017) 142.